ACS APPLIED MATERIALS & INTERFACES

Letter

www.acsami.org

One-Dimensional TiO_2@Ag Nanoarchitectures with Interface-Mediated Implementation of Resistance-Switching Behavior in Polymer Nanocomposites

Kiwon Oh, Woojin Jeon, and Sang-Soo Lee*

Photo-Electronic Hybrids Research Center, Korea Institute of Science and Technology, Seoul 136-791, Republic of Korea

ABSTRACT: A nanocomposite capable of showing a resistance-switching behavior is prepared using novel resistance-switchable fillers embedded in a polymer matrix. The filler in this study employs a conformal passivation layer of highly crystalline TiO_2 on surfaces of conductive Ag nanowires to effectively gate electron flows delivered through the conductive core, resulting in an excellent resistance-switching performance. A nanocomposite prepared by controlled mixing of the resistance-switchable nanowires with a polymer matrix successfully exhibited a resistance-switching behavior of highly enhanced reliability and a resistance on/off ratio, along with flexibility due to the presence of nanowires of a tiny amount. The advantages of our approach include a simple and low-cost fabrication procedure along with sustainable performances suitable for a resistance-switching random-access-memory application.

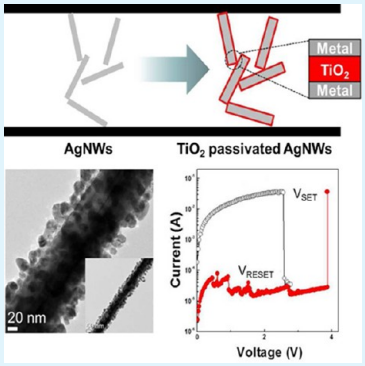

KEYWORDS: *resistance-switching random access memory, conductive nanowires, passivation, nanocomposites*

1. INTRODUCTION

Resistance-switching random access memory (RRAM) based on resistive-switching phenomena in metal/oxide insulator/metal (MIM) stack structures has been intensively researched in recent years as a promising next-generation memory candidate because of characteristics such as high operation speed, low power consumption, and nonvolatility.[1−8] Among them, several research groups have reported studies for flexible RRAM relevant to next-generation devices equipped with fully flexible microelectronic circuits.[9−14] One of the methods for fabricating a flexible RRAM is to deposit a transition-metal oxide onto a flexible substrate.[10,11,13] Although the merit of transition-metal oxide is clear for RRAM because of its high resistance ratio, endurance, uniformity, and compatibility with silicon-based device processes, that method cannot be the ultimate solution for flexible RRAM because a highly thin layer of transition-metal oxide deposited onto a flexible substrate would not be mechanically robust enough to preserve the initial properties. Another method is to use a flexible polymer that possesses resistance-switching (RS) capability.[9,12,14] However, the test using polymers capable of RS tends to exhibit some problems such as poor performance and a highly complicated synthetic process coupled with low yield.

More recently, RS phenomena in a bulk polymer nanocomposite using silver nanowires have been reported.[15,16] However, the RS behavior of the nanocomposite seems to be unstable, reversible, or irreversible by cases, which is undesirable for potential RRAM devices in that the critical issues for future memory devices are reliability, such as data retention and memory endurance.

In this study, in order to solve the aforementioned problems, we propose a RRAM material of novel concept, which is made up of the one-dimensional resistance-switchable fillers in a polymer matrix. One-dimensional RS fillers are constructed with two components: one is permanently a conductive core providing longer and faster electron transport with no use of energy to create a conductive path through device thickness, and the other is a skin layer with RS capability to gate electron flow delivered through the conductive core. Rodlike conductive fillers passivated with a transition-metal oxide layer were mixed with a polymer matrix to form a flexible nanocomposite of RS capability. The nanocomposite at the filler concentration near the percolation threshold showed proper RS behavior, and it was found out that the RS behavior originated from the one-dimensional RS fillers embedded in a polymer matrix.

2. EXPERIMENTAL SECTION

Materials. Silver nanowires (AgNWs; SLV-NW-90) were purchased from Blue Nano Inc. and purified with deionized water after vacuum filtration. AgNWs have diameters of 90 ± 20 nm and lengths of 20−60 μm. Titanium tetrachloride ($TiCl_4$) purchased from Merck was used as a precursor for titanium dioxide (TiO_2) as received. Poly(vinyl alcohol) (PVA), purchased from Sigma-Aldrich and diluted to 10 wt % solution with deionized water, was used as the polymer matrix.

Received: July 17, 2012
Accepted: September 7, 2012
Published: September 7, 2012

 © 2012 American Chemical Society

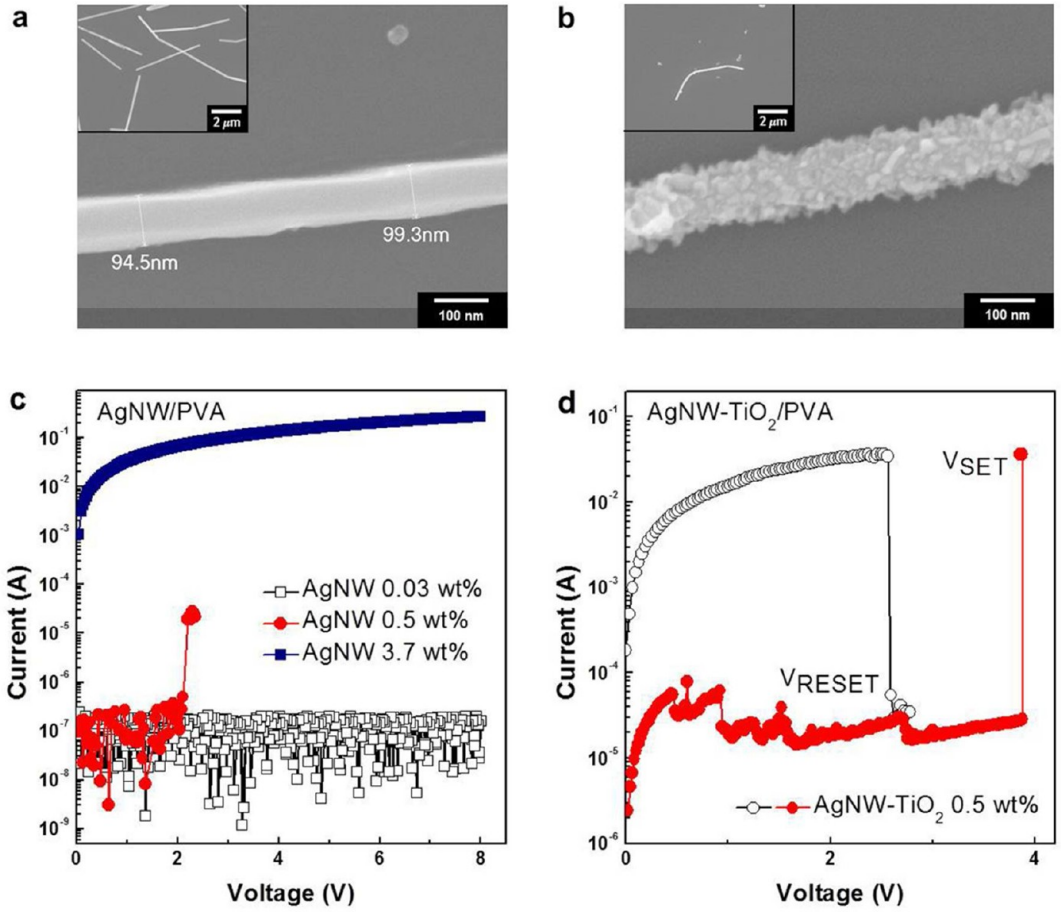

Figure 1. SEM images of (a) AgNW and (b) AgNW-TiO_2. $I-V$ curves for (c) AgNW/PVA and (d) AgNW-TiO_2/PVA nanocomposites with different filler concentrations.

Preparation of the RS Filler (AgNW-TiO_2). AgNWs were added to deionized water, and then $TiCl_4$ diluted to a 2 M solution with deionized water was carefully dropped into the solution. The resulting solution was kept at 60 °C for 8 h under constant stirring. Then, the crude product (AgNW-TiO_2) was collected by vacuum filtration, followed by rinsing with deionized water to remove the byproduct (HCl). Subsequently, AgNW-TiO_2 was dried using a freeze dryer for 24 h. Finally, AgNW-TiO_2 was heat-treated in a tubular furnace programmed at 100 °C for 1 h and then at 400 °C for 1 h under ambient atmosphere to induce crystallization of the TiO_2 layer.

Preparation of RS-Filler-Embedded Nanocomposites. AgNWs and AgNW-TiO_2 were added to the PVA solution of 10 wt % diluted by deionized water, separately. The amount of filler in the PVA solution was varied as 0.03, 0.5, and 3.7 wt %. The filler/PVA solution mixture was stirred at 80 °C for 12 h. After mixing, the filler/PVA solution mixture was degassed under vacuum conditions.

Sample Characterization. In order to fabricate a test cell for measuring RS characteristics, a platinum (Pt) bottom electrode with 100 nm thickness was sputtered on a glass substrate. Subsequently, the filler/PVA solution mixture made above was cast onto the Pt-sputtered glass substrate, followed by drying under vacuum for 12 h to form a filler/PVA nanocomposite film with a thickness of about 100 μm. As a top electrode of the cell, rectangular-shaped Ag spots with an area of 2.0 × 2.0 mm^2 were formed on the nanocomposite film. The cells made from a filler/PVA nanocomposite film were subjected to current (I)−voltage (V) measurements (Parstat 2273, Princeton Applied Research) at room temperature under ambient conditions. Morphological analyses were carried out by a field-emission scanning electron microscope (Jeol JSM 6701) and a transmission electron microscope (FEI, Tecnai G2).

3. RESULTS AND DISCUSSION

RRAM is based on RS phenomena exhibited as typical $I-V$ curves in a MIM capacitor structure of insulators.[4,5,7] The switching behaviors can be classified into two types, unipolar and bipolar, depending on the relationship between the bias sweep direction and RS. Among them, we focused on unipolar RS (URS), which is known as a thermochemical RS mechanism including "set" [switching from a high resistance state (HRS) to a low resistance state (LRS)] and "reset" (switching from an LRS to an HRS) processes, respectively. Of many materials that exhibit RS behavior,[1,17−24] we employed TiO_2[17,19,22−24] in the role of RS behavior in our system.

In order to fabricate a polymer nanocomposite of RS capability, AgNWs chosen as conductive fillers because of their high aspect ratio and excellent electrical conductivity were passivated with TiO_2. Parts a and b of Figure 1 show that the clean surface of AgNWs is well-coated by TiO_2 (AgNW-TiO_2). Then AgNW-TiO_2 was mixed with PVA chosen as the polymer matrix (AgNW-TiO_2/PVA nanocomposite), which was subjected to a performance test if RS behavior can be found. For comparison, pristine AgNWs were also mixed with PVA to form a AgNW/PVA nanocomposite. $I-V$ measurements for

dx.doi.org/10.1021/am301362f | ACS Appl. Mater. Interfaces 2012, 4, 5727−5731

nanocomposites containing AgNWs and AgNW-TiO_2 with different filler concentrations are shown in Figure 1c,d, respectively. While the nanocomposites containing pristine AgNWs of 0.03 or 3.7 wt % do not exhibit any trace of RS behavior over the scanned voltage range, RS behavior is observed when the AgNW concentration is 0.5 wt %, which is seemingly near the percolation threshold (Figure 1c). However, the resistance ratio of the AgNW/PVA nanocomposite with 0.5 wt % of AgNWs was about 10^1, and the RS behavior was irreversible, demonstrating that pristine AgNW cannot afford to show usable RS performance and reliability. On the other hand, $I-V$ curves for the AgNW-TiO_2/PVA nanocomposite with 0.5 wt % AgNW-TiO_2 show a higher resistance ratio, which was over 10^3, and a reversible RS behavior including "set" and "reset" processes (Figure 1d). These results demonstrate that the RS behavior of the AgNW-TiO_2/PVA nanocomposite originated from URS behavior and the nanocomposite has great advantages of showing a high resistance ratio and reversible RS behavior, which can be explained by a fuse–antifuse mechanism in the TiO_2 passivation layer.[22] On the basis of the mechanism, when one-dimensional RS fillers made up of a permanently conductive core (AgNWs) and a skin layer (TiO_2) with RS capability form the MIM structure in the nanocomposite, it is expected to make a conductive path because a form of filament is constructed as a soft breakdown of the TiO_2 layer by an applied electric field, which is called the "forming" process. Afterward, resistance can be abruptly increased or decreased because rupture or formation of the conductive filament takes place by an external field and thermal effect, which enables the nanocomposite to perform RS behavior.

It is worth noticing that the thickness of the TiO_2 passivation layer can be controlled, which would lead the nanocomposites to have different resistance ratios. It was found that changing the concentration of $TiCl_4$, which is a precursor of TiO_2, enables the passivation layer to be controlled. Parts a and b of Figure 2 exhibit AgNWs with a thin TiO_2 layer and a relatively thick TiO_2 layer prepared from the respective recipe employing 1 and 3 mL of $TiCl_4$. The thicknesses of the TiO_2 layer are about 10 nm using 1 mL of $TiCl_4$ and about 30 nm using 3 mL of $TiCl_4$. This implies that the crystallization of TiO_2 mainly takes place on the surface of the AgNW. Figure 2c shows the RS behavior of AgNW-TiO_2/PVA nanocomposites with different thicknesses of the TiO_2 layer. With reversible RS behavior, the AgNW-TiO_2/PVA nanocomposites have a tendency to exhibit higher resistance ratios when the TiO_2 layer is thicker. Moreover, the applied voltages for the RS behavior of the composite with a thicker TiO_2 layer were higher (2.5 and 4 V) than those of the composite with a thinner TiO_2 layer (0.5 and 1 V). These results can be attributed to the fact that the HRS of the AgNW-TiO_2/PVA nanocomposites during the "reset" process was influenced by the thickness of the TiO_2 layer, which reconfirms that the RS behavior originated from the TiO_2 layer. Combined with the fact that the resistance of a typical resistor is proportional to its thickness, it has been reported that the HRS of a thin film made up of an electric insulator (SiO_2) and a metallic particle (Pt) can be tuned by the film thickness.[25] Therefore, in our nanocomposites, the thicker TiO_2 layer, acting in the role of the thin film mentioned above, is more advantageous than the thinner TiO_2 layer when performing RS characteristics.

Transmission electron microscopy (TEM) images and selected-area diffraction (SAD) patterns acquired on the surfaces of different fillers are shown in Figure 3. As shown

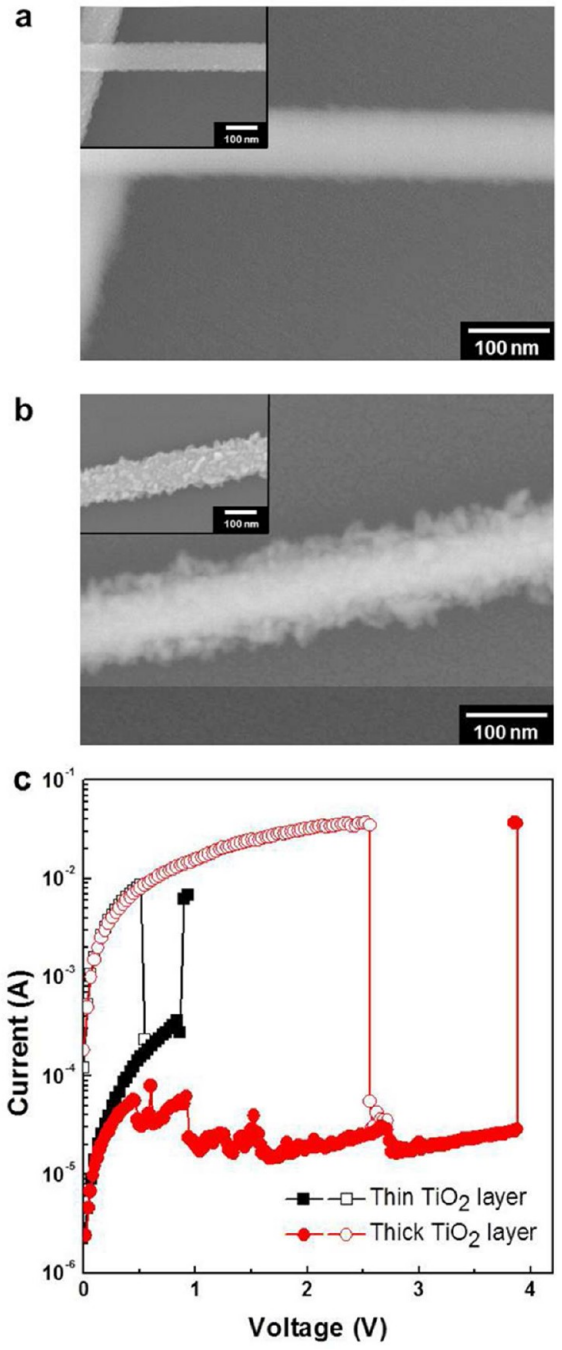

Figure 2. SEM images of (a) AgNW-thin TiO_2 and (b) AgNW-thick TiO_2. (c) $I-V$ curves for AgNW-TiO_2/PVA nanocomposites with different TiO_2 layer thicknesses. Note that AgNW-thin TiO_2 and AgNW-thick TiO_2 concentrations of the composites were 0.5 wt %.

in parts a and d of Figure 3, the pristine AgNW shows a clean and smooth surface, and the SAD pattern is typical. Ring patterns responding to the crystal structure of the TiO_2 phase, which are close to those of the anatase phase[26,27] appeared from the sample of the thin TiO_2 layer (Figure 3b,e) and increased in intensity as the thickness of the TiO_2 layer increased (Figure 3c,f), indicating that the crystal structure of TiO_2 was well-developed on the surface of AgNWs.

Figure 4a exhibits a schematic illustration of our filler/PVA nanocomposite of RS capability at the concentration of the filler near the percolation threshold. The MIM structure made

dx.doi.org/10.1021/am301362f | ACS Appl. Mater. Interfaces 2012, 4, 5727–5731

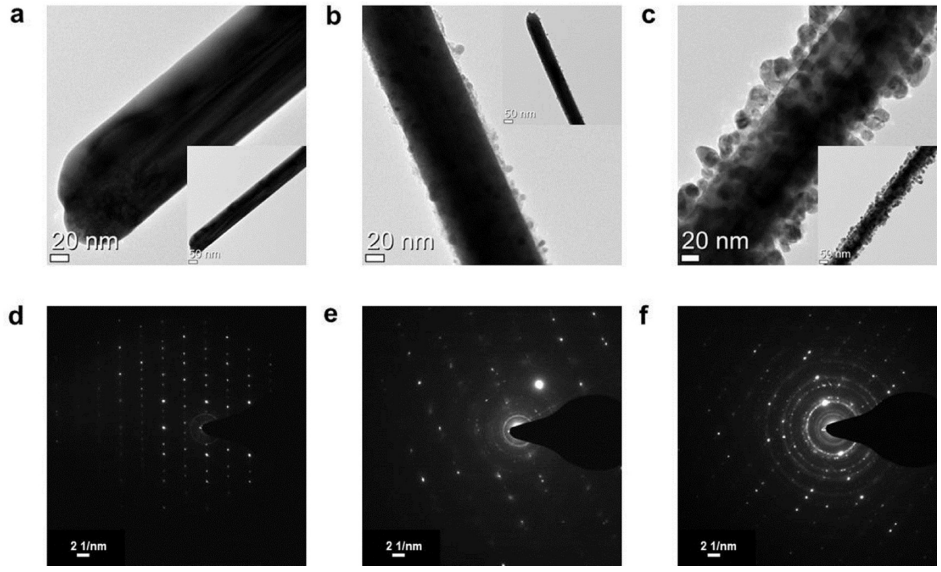

Figure 3. TEM images and the respective SAD patterns acquired on the surface of (a, d) AgNW, (b, e) AgNW-thin TiO_2, and (c, f) AgNW-thick TiO_2.

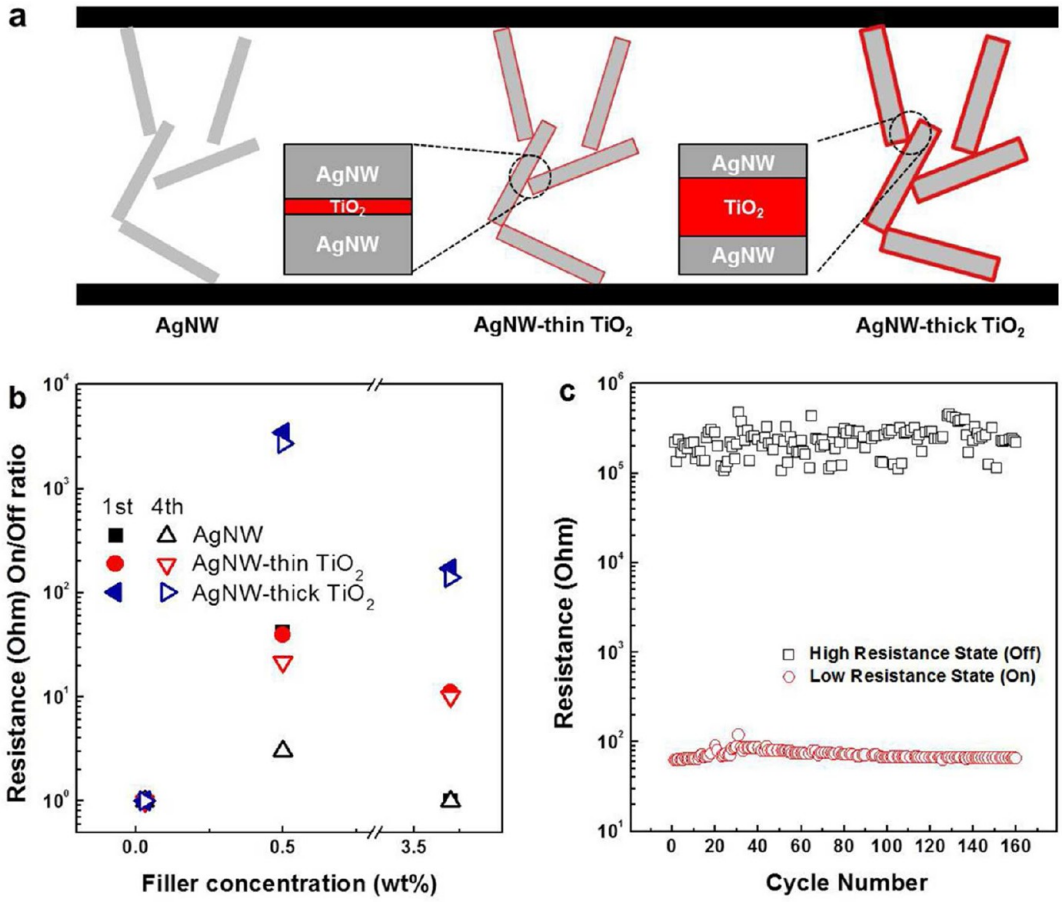

Figure 4. (a) Schematic illustration of filler/PVA nanocomposites at the concentration of the filler near the percolation threshold. Small circle regions indicate that a MIM structure in the PVA matrix exists between AgNWs with different insulating thicknesses. (b) Ratio of resistance (Ohm) on and off states for nanocomposites with different fillers, for the first (closed mark) and fourth (open mark) *I*–*V* sweeps. (c) Cyclic test on the AgNW-thick TiO_2/PVA nanocomposite with 0.5 wt % filler concentration.

up of AgNW/TiO_2/AgNW in a polymer matrix could be obtainable between adjacent AgNW-TiO_2 layers by controlling the concentration of the filler. When the conductive path through the device thickness is created, the MIM structures in the nanocomposite could be more than one, and one of the MIM structures plays a significant role in performing RS behavior because the rupture or formation of a conductive filament takes place mainly at the same location. Although the

dx.doi.org/10.1021/am301362f | ACS Appl. Mater. Interfaces 2012, 4, 5727–5731

number of MIM structures cannot be controlled and might affect the RS behavior, the results of switching tests showed a reliable performance because it is difficult to make a great difference in each test considering the size of the device and filler. To examine the reliability of the RS behavior of AgNW-TiO_2/PVA nanocomposites, successive $I-V$ scans of four cycles were performed, and a comparison of the resistance on/off ratio with each sample including AgNW/PVA, AgNW-thin TiO_2/PVA, and AgNW-thick TiO_2/PVA was tried as a function of the filler concentration. As shown in Figure 4b, exhibiting the on/off ratios for the first (closed mark) and fourth (open mark) $I-V$ sweeps with different fillers, when the concentration of the filler is 0.03 wt %, much smaller than the percolation threshold, all of the composites have high resistance without RS behavior, showing an on/off ratio of 1 during all of the scans. This is because the filler cannot construct a conductive pathway without a high enough filler concentration. When the RS filler concentration is increased to 0.5 wt %, close to the percolation threshold, both AgNW-thin TiO_2/PVA and AgNW-thick TiO_2/PVA nanocomposites exhibit stable RS behavior for all of the scans, while the RS behavior of the AgNW/PVA nanocomposite appears irreversible at the fourth scan, suggesting that the MIM structure by a passivated conductive rod in the polymer matrix can impart enhanced reliability of RS behavior to the AgNW/PVA nanocomposites.

When the concentration of the filler reaches 3.7 wt %, large beyond the percolation threshold, the AgNW/PVA nanocomposite has no RS behavior because of the permanent formation of a conducting pathway within the matrix. In the case of nanocomposites employing AgNW-TiO_2, although a slight decrease is detected at the high scan number, the on/off ratio exhibits a good reliability of the RS behavior, which becomes prominent for a thicker passivation layer, evidencing again the importance of the MIM structure.

A cyclic test on the AgNW-TiO_2/PVA nanocomposite with 0.5 wt % filler concentration is shown in Figure 4c. The composite during a cyclic test of more than 160 times exhibited a highly sustainable resistance on/off ratio of over 10^3, implying its affordable reliability as a candidate of the RS material.

4. CONCLUSIONS

We have demonstrated the novel RRAM material, which is made up of passivated conductive nanowires in a polymer matrix. The passivated nanowires/polymer nanocomposite showed highly enhanced reliability of the RS behavior and resistance on/off ratio, compared with a nanocomposite employing conductive nanowires without a passivation layer. Furthermore, we found that the thicknesses of the passivation layers could affect the resistance ratio of the of RS behavior. We believe that there is room for improvement, such as a switching speed via the use of a switching material of which the performance is tunable by formulation of constructing components of the passivation layer and their geometry of assembly. It should be noted that the concept of using a TiO_2-coated conductive component of one-dimensional structure as the resistance-switching medium performed well, even in a nonoptimized state. The advantages of our approach include a simple and low-cost fabrication procedure along with sustainable performances suitable for RRAM application.

AUTHOR INFORMATION

Corresponding Author

*E-mail: s-slee@kist.re.kr.

Notes

The authors declare no competing financial interest.

ACKNOWLEDGMENTS

This work was kindly supported by Grant 2011-0032156 from the Center for Advanced Soft Electronics under the Global Frontier Research Program of the Ministry of Education, Science and Technology, Korea, and a grant from the Seed Collaborative R&D Program funded by the Korean Research Council of Fundamental Science and Technology. S.-S.L. also appreciates support by the 2012 internal project of KIST.

REFERENCES

(1) Seo, S.; Lee, M.; Seo, D.; Jeoung, E.; Suh, D. S.; Joung, Y.; Yoo, I.; Hwang, I.; Kim, S.; Byun, I. *Appl. Phys. Lett.* **2004**, *85*, 5655.
(2) Kinoshita, K.; Tamura, T.; Aoki, M.; Sugiyama, Y.; Tanaka, H. *Appl. Phys. Lett.* **2006**, *89*, 103509.
(3) Ogimoto, Y.; Tamai, Y.; Kawasaki, M.; Tokura, Y. *Appl. Phys. Lett.* **2007**, *90*, 143515.
(4) Waser, R.; Aono, M. *Nat. Mater.* **2007**, *6*, 833.
(5) Sawa, A. *Mater. Today* **2008**, *11*, 28.
(6) Strukov, D. B.; Snider, G. S.; Stewart, D. R.; Williams, R. S. *Nature* **2008**, *453*, 80.
(7) Waser, R.; Dittmann, R.; Staikov, G.; Szot, K. *Adv. Mater.* **2009**, *21*, 2632.
(8) Muenstermann, R.; Menke, T.; Dittmann, R.; Waser, R. *Adv. Mater.* **2010**, *22*, 4819.
(9) Scott, J. C.; Bozano, L. D. *Adv. Mater.* **2007**, *19*, 1452.
(10) Gergel-Hackett, N.; Hamadani, B.; Dunlap, B.; Suehle, J.; Richter, C.; Hacker, C.; Gundlach, D. *IEEE Electron Device Lett.* **2009**, *30*, 706.
(11) Kim, S.; Moon, H.; Gupta, D.; Yoo, S.; Choi, Y. K. *IEEE Trans. Electron Devices* **2009**, *56*, 696.
(12) Kim, T. W.; Choi, H.; Oh, S. H.; Wang, G.; Kim, D. Y.; Hwang, H.; Lee, T. *Adv. Mater.* **2009**, *21*, 2497.
(13) Jeong, H. Y.; Kim, Y. I.; Lee, J. Y.; Choi, S. Y. *Nanotechnology* **2010**, *21*, 115203.
(14) Park, S.; Lee, T. J.; Kim, D. M.; Kim, J. C.; Kim, K.; Kwon, W.; Ko, Y. G.; Choi, H.; Chang, T.; Ree, M. *J. Phys. Chem. B* **2010**, *114*, 10294.
(15) White, S. I.; Vora, P. M.; Kikkawa, J. M.; Winey, K. I. *Adv. Funct. Mater.* **2011**, *21*, 233.
(16) White, S. I.; Vora, P. M.; Kikkawa, J. M.; Fischer, J. E.; Winey, K. I. *J. Phys. Chem. C* **2010**, *114*, 22106.
(17) Choi, B.; Jeong, D.; Kim, S.; Rohde, C.; Choi, S.; Oh, J.; Kim, H.; Hwang, C.; Szot, K.; Waser, R. *Appl. Phys.* **2005**, *98*, 033715.
(18) Lee, D.; Choi, H.; Sim, H.; Choi, D.; Hwang, H.; Lee, M. J.; Seo, S. A.; Yoo, I. *IEEE Electron Device Lett.* **2005**, *26*, 719.
(19) Rohde, C.; Choi, B. J.; Jeong, D. S.; Choi, S.; Zhao, J. S.; Hwang, C. S. *Appl. Phys. Lett.* **2005**, *86*, 262907.
(20) Sim, H.; Choi, D.; Lee, D.; Seo, S.; Lee, M. J.; Yoo, I. K.; Hwang, H. *IEEE Electron Device Lett.* **2005**, *26*, 292.
(21) Villafuerte, M.; Heluani, S.; Juarez, G.; Simonelli, G.; Braunstein, G.; Duhalde, S. *Appl. Phys. Lett.* **2007**, *90*, 052105.
(22) Jeong, D. S.; Schroeder, H.; Breuer, U.; Waser, R. *J. Appl. Phys.* **2008**, *104*, 123716.
(23) Kwon, D. H.; Kim, K. M.; Jang, J. H.; Jeon, J. M.; Lee, M. H.; Kim, G. H.; Li, X. S.; Park, G. S.; Lee, B.; Han, S. *Nat. Nanotechnol.* **2010**, *5*, 148.
(24) Kim, K. M.; Song, S. J.; Kim, G. H.; Seok, J. Y.; Lee, M. H.; Yoon, J. H.; Park, J.; Hwang, C. S. *Adv. Funct. Mater.* **2011**, *21*, 1587.
(25) Choi, B. J.; Chen, A. B. K.; Yang, X.; Chen, I. W. *Adv. Mater.* **2011**, *23*, 3847.
(26) Bose, P.; Pradhan, S.; Sen, S. *Mater. Chem. Phys.* **2003**, *80*, 73.
(27) Deng, Q.; Xia, X.; Guo, M.; Gao, Y.; Shao, G. *Mater. Lett.* **2011**, *65*, 2051.